NASA TECHNICAL MEMORANDUM

NASA TM X-2281

NASA TM X-2281

POTENTIAL OF METHANE-FUELED SUPERSONIC TRANSPORTS OVER A RANGE OF CRUISE SPEEDS UP TO MACH 4

by John B. Whitlow, Jr., and Gerald A. Kraft

Lewis Research Center
Cleveland, Ohio 44135

NATIONAL AERONAUTICS AND SPACE ADMINISTRATION • WASHINGTON, D. C. • MAY 1971

1. Report No.	2. Government Accession No.	3. Recipient's Catalog No.
NASA TM X-2281		

4. Title and Subtitle	5. Report Date
POTENTIAL OF METHANE-FUELED SUPERSONIC TRANSPORTS OVER A RANGE OF CRUISE SPEEDS UP TO MACH 4	May 1971
	6. Performing Organization Code

7. Author(s)	8. Performing Organization Report No.
John B. Whitlow, Jr., and Gerald A. Kraft	E-6088
	10. Work Unit No. 720-03
9. Performing Organization Name and Address Lewis Research Center National Aeronautics and Space Administration Cleveland, Ohio 44135	11. Contract or Grant No.
	13. Type of Report and Period Covered
12. Sponsoring Agency Name and Address National Aeronautics and Space Administration Washington, D. C. 20546	14. Sponsoring Agency Code

15. Supplementary Notes

16. Abstract

A major factor restricting currently proposed SST's to a maximum cruise speed of Mach 2.7 is the limited heat sink capacity of kerosene-type fuels. Higher speeds may be possible with cryogenic liquid methane, which has up to seven times the heat sink and can be economically obtained from natural gas. In this analysis, methane was considered as the fuel for airplanes designed to cruise at speeds up to Mach 4. When a comparison was made at Mach 2.7 with a conventionally fueled SST, the use of methane improved both range and direct operating cost (DOC) by about 11 percent. Little range improvement was obtained by cruising faster than Mach 2.7, although certain assumptions made in this study should produce somewhat optimistic results at the higher speeds. Range peaked near Mach 3 and decreased from 6 to 13 percent as cruise speed was increased to Mach 4. The block time reductions obtained with higher cruise speeds are beneficial to DOC. Most of the possible DOC improvement was obtained by a speed increase to Mach 3.2, where a 20-minute time saving produced 7 percent improvement in DOC.

17. Key Words (Suggested by Author(s))	18. Distribution Statement
SST Methane	Unclassified - unlimited

19. Security Classif. (of this report)	20. Security Classif. (of this page)	21. No. of Pages	22. Price*
Unclassified	Unclassified	40	$3.00

* For sale by the National Technical Information Service, Springfield, Virginia 22151

CONTENTS

POTENTIAL OF METHANE-FUELED SUPERSONIC TRANSPORTS OVER A RANGE OF CRUISE SPEEDS UP TO MACH 4

by John B. Whitlow, Jr., and Gerald A. Kraft

Lewis Research Center

SUMMARY

Since cruise flight efficiency is proportional to Mach number (among other factors), there is an incentive to increase the cruise speed of the supersonic transport beyond the currently proposed maximum of Mach 2.7. A major factor limiting the cruise speed to Mach 2.7 is the heat sink capacity of conventional kerosene-type fuels. Cryogenic liquid methane, with up to seven times the heat sink of kerosene, is an economical fuel that can be obtained from natural gas. In this analysis, methane was considered as the fuel for a 3 170 000-newton (712 000-pound) airplane designed to carry a payload of 285 passengers at cruise speeds up to Mach 4.0. Only afterburning turbojet engines were considered. Two different combinations of turbine-inlet and afterburner temperature were studied. Design compressor pressure ratio and airflow were optimized to maximize range for each mission. Podded engine weight was assumed to increase with rises in design compressor pressure ratio and airflow as well as cruise Mach number.

When a comparison was made at Mach 2.7 with a conventionally fueled SST, the use of methane improved both range and direct operating cost (DOC) about 11 percent. Little range improvement was obtained by cruising faster than Mach 2.7, although certain assumptions made in this study (e.g., constant airframe weight, cost, and turbine cooling bleed percentage) should produce somewhat optimistic results at the higher speeds. Range peaked near Mach 3 and decreased from 6 to 13 percent as cruise speed was increased to Mach 4. The block time reductions obtained with higher cruise speeds are beneficial to DOC. Most of the possible improvement in DOC was obtained by a speed increase to Mach 3.2, where a 20-minute timesaving produced a 7 percent improvement in DOC, compared with that obtained at Mach 2.7. If the Mach 3.2 methane airplane is compared to the Mach 2.7 kerosene-fueled SST, DOC reductions of 17 to 18 percent are possible.

INTRODUCTION

Ever since the beginning of flight by man, he has striven to increase his travel speed between any two points. Not only will his trip time be reduced, but there is a good possibility that the cruise flight efficiency (sometimes called Breguet factor) will also increase since it is proportional to the Mach number (among other factors). An improved flight efficiency will be reflected in range/payload improvements. Both the range/payload improvements and the higher block speed will reduce the direct operating cost (DOC). Hence, there is certainly a tangible incentive for investigating higher cruise speeds.

Mach 2.7 is the maximum cruise speed for any of the currently proposed commercial supersonic transport (SST) designs. One of the considerations which tends to restrict the SST to Mach 2.7 is the limited heat sink capability of conventional kerosene-type fuels. As additional heat resulting from cruise at higher Mach numbers is dumped into conventional fuels, they begin to decompose, leaving gummy deposits in the fuel lines and fuel heat exchangers. With kerosene-type fuels, practically all of the heat sink available is used at Mach 2.7 cruise to absorb the heat discharged by the cabin environmental control system and the engine oil cooling system. In order to take advantage of the possible benefits of higher cruise speeds in an SST, then, an economical fuel with a higher heat sink is required.

Reference 1 indicates that liquid methane may prove to be a satisfactory fuel for an SST designed to cruise in the currently proposed Mach 2.7 speed regime. In addition to a heat of combustion 13 percent higher than that of conventional fuels, it has a heat sink capacity up to seven times as great. In past studies (e.g., refs. 1 and 2), the higher heat sink of methane led to consideration of higher turbine inlet temperatures or greater turbine blade life expectancy at Mach 2.7 by using methane-air heat exchangers to cool the compressor discharge air in the turbine cooling circuit. In the present study, however, the extra heat sink capacity of methane will be used to permit cruise at higher Mach numbers. Cruise at speeds up to Mach 4 will be considered. It is expected that an increase in cruise speed from Mach 2.7 to Mach 4.0 will permit a time saving of about 40 minutes for a 7408-kilometer (4000-n-mi) design range. The purpose of this study is to determine what, if any, additional benefits can be obtained in terms of range and DOC improvements.

Liquid methane is, unfortunately, only about half as dense as conventional kerosene-type fuels. Therefore, regardless of the design cruise speed, it may be difficult to find enough fuel storage volume on board the airplane if reasonable range/payload characteristics are to be obtained. In reference 1, the relative thick and blunt-nosed subsonic-leading-edge wings of that SCAT 15 F configuration could hold a considerable amount of fuel. In the present study, however, sharp, supersonic-leading-edge wings are necessary

for efficient cruise at higher speeds with a relatively high aspect ratio delta wing. (High aspect ratios lead to better subsonic aerodynamics; the SST must have acceptable subsonic as well as supersonic characteristics.) The low-volume wings, then, made the choice of a larger-diameter, high-volume fuselage essential. Even with the supersonic-leading-edge wing, some fuel is stored in the thicker inboard portions, but most is stored in the fuselage - both under and aft of the passengers.

Takeoff gross weight and payload are fixed while range is allowed to vary as the figure of merit in this study. Estimates of DOC are also computed over the cruise-speed spectrum from Mach 2.2 to Mach 4.0. The takeoff wing loading and the minimum allowable thrust-to-gross-weight ratio are fixed at values that yield adequate takeoff performance. Airport and community jet noise constraints were ignored in this preliminary study. If the benefits of higher speed are significant, the penalties that would be incurred by meeting noise constraints can then be assessed.

The engines are also sized to meet minimum transonic and supersonic thrust margin requirements over a fixed flight path which was chosen without regard to any sonic boom constraint. Although sonic boom constraints were not allowed to affect the range or DOC calculations, the far-field sonic boom at the beginning of cruise was, nevertheless, calculated. This was done to determine if the higher cruise altitude and the lower lift coefficient associated with higher cruise speeds might combine to appreciably reduce the sonic boom at the beginning of cruise.

SYMBOLS

A	wing aspect ratio, b/c
b	wing span, m (ft)
C_{fg}	nozzle gross thrust coefficient
C_D	drag coefficient
C_L	lift coefficient
C_{L_o}	lift coefficient at minimum drag
c	wing mean chord, m (ft)
D	drag, N (lb)
ECS	environmental control system
F	thrust, N (lb)
K	coefficient of induced drag due to lift, $C_{D_i}/(C_L - C_{L_o})^2$

K_M engine weight factor for Mach number

K_p engine weight factor for compressor pressure ratio

L lift, N (lb)

M Mach number

N shaft rotational speed, rev/min

P total pressure, N/m^2 (lb/ft^2)

S wing planform area, m^2 (ft^2)

T total temperature, K (^oR)

W_a engine airflow, N/sec (lb/sec)

W_e podded weight of four engines, N (lb)

W_g airplane takeoff gross weight, N (lb)

W_{hx} weight of methane-air heat exchangers for four engines, N (lb)

β Mach number parameter, $\sqrt{M^2 - 1}$

δ pressure parameter, P/101 200 (P/2116)

$\eta_{c_{ad}}$ compressor adiabatic efficiency

θ temperature parameter, T/288 (T/519)

Subscripts:

des design

i induced

max maximum

min minimum

ref reference

0 free stream station

1 compressor inlet station

2 compressor discharge station

4 turbine inlet station

METHOD OF ANALYSIS

Configuration

The delta-wing with aft-tail configuration shown in figure 1 was chosen for this study. The delta wing was chosen for its high structural efficiency and thus relatively low weight. Both leading- and trailing-edge flaps provide high subsonic lift with a moderately high wing loading (e.g., wing loading at takeoff W_g/S_{ref} is 4430 N/m^2 or 92.5 lb/ft^2). Longitudinal control and trim are provided by the movable horizontal tail. The relatively high wing aspect ratio of 2.5 (i.e., high for a high supersonic speed) was chosen to minimize the subsonic vortex drag due to lift, since good subsonic performance is almost as important to the SST as good supersonic performance. For a delta wing of this aspect ratio, a supersonic leading edge is a necessity, even for the lowest cruise speed considered in this study - Mach 2.2. At this speed with an aspect ratio of 2.5, the component of the free stream velocity normal to the leading edge of a pure delta planform would be Mach 1.17. According to reference 3, as an arbitrary rule of thumb, a subsonic-leading-edge wing should not be designed for a normal Mach number greater than 0.7. The modified delta wing used on the airplane of this study has an inboard sweepback angle of 64.6°. At Mach 2.2, the Mach number normal to the leading edge is 0.94, which is still greater than the Mach 0.7 criterion for a subsonic leading edge.

For the airplane of this study, as shown in figure 1, the 3-percent thickness to chord ratio of the inboard portion of the wing leading edge was necessary to provide enough thickness to store the wheels and a significant amount of fuel. A leading-edge sweepback angle of 64.6° is used on this inboard portion so that at Mach 4, the maximum cruise speed considered, a normal free stream Mach number component of 1.72 is obtained. This value of normal Mach number is the same as that of the Boeing 2707-300 which has the same thickness to chord ratio (0.03) and is designed for cruise at Mach 2.7 with a wing sweepback of 50.5° (ref. 4).

The outboard portion of the leading edge of the wing of the airplane of this study is unswept somewhat to 50.5° to obtain an overall wing aspect ratio of 2.5. The thickness to chord ratio of this portion, however, is reduced to keep the maximum Mach number over the suction surface normal to the leading edge no higher than that over the more highly swept inboard portion. No fuel storage is contemplated in the thinner outboard portion of the wing. The shaded area of the inboard portion of the wing of figure 1 indicates a fuel storage location equivalent to about 67.9 cubic meters (2400 ft^3), or about 17.4 percent of the total available fuel storage volume on the entire airplane. Separate fuel tanks (rather than integral) covered with fiber glass insulation were chosen to contain the liquid methane.

The use of relatively low-volume, supersonic-leading-edge wings necessitates the selection of a high-volume fuselage to hold the low-density methane fuel. In addition, a large payload capacity (285 passengers) was chosen in an attempt to keep the DOC (per seat mile) low. The combined fuel and payload requirements are satisfied by a fuselage that is 91.4 meters (300 ft) long and 3.96 meters (156 in.) wide at its maximum diameter. Fuel is stored in separate tanks both under and aft of the passengers, as indicated by the shaded area of figure 1. The fuel storage volume in the fuselage is 323 cubic meters (11 400 ft^3), or about 82.6 percent of the total fuel capacity of 391 cubic meters (13 800 ft^3). A baggage and cargo area is shown aft of the passengers and ahead of the rear full-diameter fuel tanks. This storage area has a capacity of 47.9 cubic meters (1690 ft^3), which is sufficient for 0.1415 cubic meter (5 ft^3) per passenger with 7.50 cubic meters (265 ft^3) left over for bulk cargo. Figure 2 shows a typical fuselage section with six-abreast seating and fuel storage under the floor. (Tankage details are omitted.)

The takeoff gross weight of the methane-fueled airplanes was fixed at 3 170 000 newtons (712 000 lb) - a value which calculations showed would produce acceptable intercontinental ranges. Takeoff wing loading was fixed at 4430 newtons per square meter (92.5 lb/ft^2) - more than 5 percent below that of the heavier Boeing 2707-300. The minimum takeoff thrust to gross weight ratio of 0.327 and the wing aspect ratio of 2.5 are approximately the same as for the Boeing 2707-300. The airplane of this study, therefore, has a lower wing loading than the Boeing airplane and thus should have better takeoff performance.

Mission

The climb and acceleration flight path, in altitude and Mach number coordinates, was fixed in this study as shown in figure 3. Sonic boom and jet noise constraints were ignored in the selection of this path. Altitude was increased with Mach number from Mach 2 to Mach 4 to maintain a constant dynamic pressure (at 37 000 N/m^2 or 773 lb/ft^2) to prevent exceeding structural limits at high Mach numbers. Weight, time, and range were computed at frequent intervals along this path by solving the equations of motion in an iterative calculation procedure in which a high-speed digital computer was used. An optimum initial Breguet cruise altitude was chosen to maximize range. If necessary, horizontal cruise was maintained until the slowly rising optimum Breguet flight path was intercepted. Letdown time and range were assumed to increase with cruise Mach number according to the schedule shown in figure 4.

A reserve fuel allowance included for all missions considered is as follows: (1) Extra fuel equal to 7 percent of the mission fuel; (2) fuel for a 483-kilometer (261-n-mi)

cruise to an alternate airport at the final supersonic cruise altitude and Mach number; (3) fuel for a 30-minute hold at Mach 0.5 at an altitude of 4572 meters (15 000 ft).

Range was allowed to vary as the figure of merit for missions having design cruise speeds of Mach 2.2, 2.7, 3.5, and 4.0. Takeoff gross weight at 3 170 000 newtons (712 000 lb) and payload at 265 000 newtons (59 600 lb) were fixed throughout the study. This payload corresponds to the weight of 285 passengers and their baggage at 930 newtons (209 lb) per passenger.

Engines

Afterburning turbojets were the only engines considered in this study. It was felt that superior thermodynamic performance would be obtained over the entire Mach number spectrum considered if the design compressor pressure ratio was optimized for each mission. Therefore, calculations were made for design compressor pressure ratios of 4, 6, 8, and 10 for each mission for cruise Mach numbers from 2.2 to 4.0. Two turbine-inlet and afterburner temperature combinations were considered. The low-temperature combination consists of a turbine-inlet temperature of 1204° C (2200° F) and an afterburner temperature of 1532° C (2790° F). The high-temperature combination consists of a turbine-inlet temperature of 1538° C (2800° F) and an afterburner temperature of 1949° C (3540° F).

Turbine cooling. - A methane-air heat exchanger was used in the turbine cooling circuit to cool the compressor discharge air bled to the turbine. Cold liquid methane fuel on its way to the burners was used to cool the bleed air which enters the heat exchanger at the compressor discharge temperature. This precooling of the turbine cooling bleed air was essential beyond Mach 2.7 for the low-temperature engines. For the higher turbine-inlet and afterburner temperature combination, the precooling was essential for the entire cruise speed spectrum considered. For the conventionally fueled Mach 2.7 airplane of this study, of course, no precooling was used because of the limited heat sink of kerosene-type fuels. Hence, the turbine-inlet temperature of this airplane was limited to 1204° C (2200° F).

Air bled from the compressor discharge for turbine cooling was fixed at 10 percent of the compressor airflow for both turbine-inlet and afterburner temperature combinations. It was assumed that no work recovery was obtained from this bleed air as it passed through the turbine and remixed with the gases in the main stream. In actuality, some work recovery is obtained from the bleed air. A true bleed somewhat greater than 10 percent would yield equivalent cycle performance results. The 10-percent bleed figure as used in this report is termed "bleed chargeable to the cycle" and is somewhat less than the actual bleed. Unless improved cooling schemes are devised, the engines

with higher turbine-inlet and afterburner temperatures will produce higher metal temperatures in these components since in this report the amount of cooling air is not increased with gas temperature.

As the cruise speed of the methane-fueled airplanes is increased beyond Mach 2.7, the compressor discharge air, of course, becomes hotter as long as the compressor design pressure ratio remains unchanged. The metal temperatures then also become hotter unless the methane-air heat exchangers are allowed to increase in size or improved cooling techniques are devised. No provision was made in the engine weight calculations for increases in heat exchanger weight with design cruise Mach number. Hence, the range calculated for cruise Mach numbers at the high end of the spectrum (i.e., near Mach 4) will be somewhat optimistic.

The desired amounts of precooling required for the compressor discharge bleed air were not calculated in this preliminary study. In the thermodynamic cycle calculations, the enthalpy of the bleed air prior to mixing after being returned to the main stream was always assumed to be equal to that of the compressor discharge air. Likewise, the enthalpy of the methane fuel entering the main burner was always assumed to be the same as that of the liquid methane in the tanks. In other words, the methane-air heat exchanger, when used, was ignored thermodynamically. If the thermodynamic system is defined as containing the engines, heat exchangers, and fuel tanks, this heat exchange if calculated is internal to the system and should not affect the interaction of the system with the surroundings. The interaction of the system with its surroundings is measured in terms of thrust and specific fuel consumption. These quantities should not be affected by ignoring a heat transfer internal to the system. Measurements of properties at stations internal to the system, however, may change if the internal transfer of energy is taken into account. Specifically, the nominal values of turbine-inlet temperature expressed in this report may be somewhat understated if the bleed air precooling requirements are severe.

Compressor and turbine matching. - Since sea-level-static design compressor pressure ratios ranging from 4 to 10 were considered, it was necessary to use several compressor maps, the extremes of which are illustrated in figure 5. These maps were scaled from two basic maps - one for the low-pressure compressors below a pressure ratio of 8 and one for the high-pressure compressors with a pressure ratio of 8 or above. A compressor map for a design pressure ratio of 4 is shown in figure 5(a), while a map for a design pressure ratio of 10 is shown in figure 5(b). The operating line is also drawn on these maps, together with the operating points for the particular cruise speeds considered in this study. These operating lines are the result of matching the compressor with its driving turbine to satisfy the relations involving flow continuity and power balance. The turbine-inlet temperature and shaft speed N were held fixed at their sea-level-static design values, and nozzle throat area was allowed to vary in determining the

location of these lines. The procedures used are similar to those described in reference 5.

Fixed-point operation on the compressor map is maintained at a particular Mach number as long as turbine-inlet temperature remains at its design value. This is true even though the afterburner temperature may vary from its design value. In supersonic cruise, this is the situation that usually occurs since thrust requirements are such that a reduced level of afterburning is needed with turbine-inlet temperature maintained at its design value. For some Mach 2.2 cruise cases, though, it may be necessary to reduce the turbine-inlet temperature below its design value because of the low thrust requirements. Part-power operation would then be obtained at a fixed value of corrected airflow at the compressor face. As turbine-inlet temperature is reduced, the compressor pressure ratio and shaft speed fall. Fixing the airflow during part-power supersonic cruise prevents an increase in inlet bypass drag which would occur in other operating modes. A variable-area primary exhaust nozzle permits this operational flexibility.

During subsonic hold at Mach 0.5 and 4572 meters (15 000 ft) altitude, part-power operation was obtained at reduced turbine-inlet temperature by allowing the uncorrected shaft speed N to decrease along the full-power operating line. The increase in inlet bypass drag with reductions in engine airflow is ignored. At the low thrust levels required for hold, better compressor efficiencies are obtained by remaining on the full-power operating line than by trying to maintain constant airflow operation. Also, there are mechanical limits to the amount of primary nozzle area variation that can be obtained. Remaining on the full-power operating line at low part-power thrust settings minimizes this area variation.

Other engine design characteristics and sizing criteria. - Sea-level-static design characteristics which remained constant for all the engines considered are as follows:

Compressor adiabatic efficiency = 0.828
Turbine adiabatic efficiency = 0.903
Primary combustor efficiency = 0.99
Afterburner combustor efficiency = 0.90
Pressure ratio across primary burner = 0.934
Afterburner dry pressure loss = dynamic pressure at afterburner station

The engines were sized to provide a takeoff thrust to gross weight ratio of at least 0.327 and a transonic and supersonic climb and acceleration thrust-drag ratio of at least 1.3 in a U.S. standard atmosphere. The engines were made larger than required for these minimum standards if range could be increased by so doing.

Inlets and nozzles. - Axisymmetric translating centerbody inlets with cowl throat and bypass doors were chosen for the engines of this study. During takeoff, the centerbody is extended, the throat doors are closed, and the takeoff doors downstream of the

throat are opened. During climb and acceleration up to Mach 1.7, the centerbody is in its fully extended position for external compression and the throat doors are open for increased flow area to satisfy engine demand. Beyond Mach 1.7, the centerbody is retracted for external-internal compression and the throat doors are closed. The inlet pressure recovery (P_1/P_0) schedule used for all engines is shown plotted against Mach number in figure 6. The cusp in the pressure recovery curve at Mach 1.7 indicates the shift in operating mode from external to external-internal compression. Up to Mach 2.7, the pressure recovery schedule is similar to that used for the Boeing 2707-300 (ref. 6). From Mach 2.7 to Mach 4.0, the slope increased negatively until it is about parallel with, although still above, the Military Specification 5008B recovery schedule. The Military Specification schedule at speeds above Mach 1 is given by

$$\frac{P_1}{P_0} = 1.0 - 0.075\,(M_o - 1.0)^{1.35}$$

Inlet drag results from a mismatch between the amount of air the engine demands and the amount the inlet could supply at various flight conditions. The supply available usually exceeds the demand except at the design cruise speed. The inlet drag is composed of the spillage, bypass, and centerbody and cowl bleed drags.

The spillage drag results from air being spilled around the cowl lip at supersonic speeds less than design because of the shock from the centerbody being positioned ahead of the cowl lip. At design cruise speed, the shock moves back to the cowl lip and no spillage occurs. Even after some of the air is spilled at Mach numbers less than design, more air is swallowed by the inlet than is demanded by the engine. This excess air is dumped overboard through bypass doors in the inlet cowl, thus creating additional drag. To maintain flow through the inlet, part of the boundary layer is bled off around the centerbody surface and inner cowl surface. This bleed is eventually dumped to create additional drag.

The inlet drag coefficient for all four engines based on wing planform area was assumed to vary with Mach number as shown in figure 7. A family of curves is shown since a different schedule is required for each cruise Mach number. The drag at the maximum Mach number on each of the curves is the result of centerbody and cowl bleed; spillage and bypass are zero. Spillage and bypass drag predominate, however, as Mach number is reduced below the maximum along each of the curves. The inlet drag coefficient of figure 7 is added to the airframe drag coefficient, to be discussed later, to obtain the total airplane drag coefficient. The curves of inlet drag coefficient are for engines having sea-level-static design corrected airflow of 2970 newtons per second (666 lb/sec) per engine. To obtain the inlet drag coefficient for other engine sizes, the coefficient read from figure 7 must be multiplied by the quotient of the new airflow

divided by the reference airflow of 2970 newtons per second (666 lb/sec).

The exhaust nozzles are assumed to be of the ejector type with secondary flow from the inlet boundary layer bleed air and tertiary flow from blow-in doors. The schedule of nozzle gross thrust coefficient as a function of Mach number used in this study is shown in figure 8. This coefficient includes the estimated nozzle boattail drag. The solid line represents the full-power climb and acceleration schedule of thrust coefficient. It is similar to one that might be obtained for an SST up to Mach 2.4, but from this point up to Mach 4.0 the thrust coefficient was maintained at its Mach 2.4 value (0.972) because of a lack of available data. At supersonic cruise speeds, the nozzles are underexpanded at maximum thrust. As thrust was reduced for cruise, the nozzle throat area was reduced while the exit area remained wide open, thereby increasing the area ratio and permitting more complete expansion inside the nozzle. This more complete internal expansion is reflected by an increase in the thrust coefficient to 0.978, as indicated by the circled points in figure 8. The thrust coefficient at part-power hold (broken line, fig. 8) was assumed to vary from 0.958 to 0.910 as a function of thrust setting, the lower values being obtained at lower thrust settings. This is because the nozzle becomes more overexpanded as thrust is reduced during hold.

Podded weight. - The podded weight of four afterburning turbojets was computed empirically:

$$W_e = \left[11\,200\,K_M(16.65\,K_p + 5.9) + W_{hx}\right] \times \left[\frac{\left(W_a \frac{\sqrt{\theta}}{\delta}\right)_{1,\mathrm{des}}}{11\,200}\right]^{1.2} \qquad \left(\frac{\mathrm{N}}{\mathrm{sec}}\right)$$

$$= \left[2520\,K_M(16.65\,K_p + 5.9) + W_{hx}\right] \times \left[\frac{\left(W_a \frac{\sqrt{\theta}}{\delta}\right)_{1,\mathrm{des}}}{2520}\right]^{1.2} \qquad \left(\frac{\mathrm{lb}}{\mathrm{sec}}\right) \qquad (1)$$

The factor K_M is designed to correct the podded engine weight for changes in design cruise Mach number. The schedule of K_M used in this study is shown plotted against design cruise Mach number in figure 9(a). This schedule is a collection of unpublished empirical data obtained from engine and airframe manufacturers. It shows that engines designed for higher supersonic cruise speeds tend to be heavier than those for subsonic or low-supersonic speeds. The engine weights are heavier for the higher design speeds because of the higher air stagnation temperatures and pressures. These higher temperatures and pressures tend to more severely stress the engine components ahead of the primary burner. To reduce the stress level to acceptable values, these

components must be made heavier. A K_M curve similar to the one used in this study appears in reference 7. It is a correction for the bare engine weight only, however, and thus does not account for increases in inlet length and complexity as Mach number increases. Its slope is about 40 percent less than the slope used for the curve of this study.

The factor K_p is used in equation (1) to correct the engine weight for changes in the sea-level-static design compressor pressure ratio. The schedule of K_p used in this study is reproduced from reference 8 and is shown plotted against design pressure ratio in figure 9(b). Higher design compressor pressure ratios tend to increase the number of stages required and the maximum stress levels in the latter stages. Hence, the tendency is toward heavier weight as design pressure ratio is increased.

The heat exchanger weight and engine airflow in equation (1) are totals for all four engines. The total heat exchanger weight used here was 5790 newtons (1300 lb) for the low-turbine-inlet-temperature engines and 7560 newtons (1700 lb) for the high-temperature engines. These are the same heat exchanger weights that were used in reference 1 at these turbine-inlet temperatures. When the weight of the kerosene-fuel engines was computed, the heat exchanger weight term was dropped since the turbine cooling air was not precooled prior to entering the turbine. The previous weight equation is of the same form as the one that appears in the appendix of reference 8, but numerical values of the terms have been changed to reflect the latest available data. No change was made in engine weight at a given airflow for an increase in design turbine-inlet or afterburner temperature except for the slight increase in turbine cooling heat exchanger weight.

In this study, typical sea-level-static thrust to podded-engine weight ratios for optimized engines are 4.3 for a low-turbine-inlet-temperature engine designed to cruise at Mach 2.2, and 5.0 for a high-turbine-inlet-temperature engine designed to cruise at Mach 4.0. For the optimized Mach 2.7 cruise engines, increasing the turbine-inlet temperature from 1204° to 1538° C (2200° to 2800° F) causes the thrust to weight ratio to rise from 4.3 to 5.3.

Aerodynamics

It was assumed that the airframe drag coefficient C_D at any Mach number was a parabolic function of the lift coefficient C_L as described by

$$C_D = C_{D_{min}} + \left[\frac{C_{D_i}}{\left(C_L - C_{L_o}\right)^2}\right]\left(C_L - C_{L_o}\right)^2$$

where $C_{D_{min}}$, $C_{D_i}/\left(C_L - C_{L_o}\right)^2$, and C_{L_o} are functions of Mach number as shown in figure 10. The reference area S_{ref} on which these coefficients are based is the wing planform area, which was fixed at 715 square meters (7700 ft^2) in this study. The $C_{D_{min}}$ schedule shown in figure 10(a) is typical of what might be expected for this airplane for the climb and acceleration flight profile used in this study and shown in figure 3. Excursions from this flight path (e.g., during cruise or hold) introduce some change in this coefficient due to the influence of Reynolds number on the frictional drag coefficient. The $C_{D_{min}}$, which is the sum of the frictional and pressure drag coefficients, includes the nacelle friction and pressure drag, but not the engine inlet-spillage or nozzle-boattail drags. They are handled separately since they, like thrust, are a function of engine size. The component of $C_{D_{min}}$ chargeable to the nacelles was fixed even though engine size was varied because of the unknown effect of the interference drag between the nacelles and airframe. The induced drag due to lift $C_{D_i}/\left(C_L - C_{L_o}\right)^2$ schedule assumed in this study is the solid curve in figure 10(b). The broken line in this figure is a plot of

$$\frac{C_{D_i}}{\left(C_L - C_{L_o}\right)^2} = \left(1 + \frac{1}{8}\beta^2 A^2 \frac{1}{\pi A}\right)$$

which is a theoretical representation of the drag-due-to-lift coefficient for a slender, thin-delta wing with no favorable leading edge suction forces (ref. 9). Since the wing planform of the airplane of this study is a modified delta, the fact that the curve used in this study (solid curve, fig. 10(b)) lies below the theoretical delta plot indicates that somewhat optimistic lift-drag ratios (L/D) may be obtained at the higher Mach numbers. This exemplifies the philosophy of this report, which is to try to maximize or set an upper bound to the benefits that may be obtained from a higher cruise speed.

The maximum lift-drag ratio $(L/D)_{max}$ may be calculated from

$$\left(\frac{L}{D}\right)_{max} = \frac{1}{2\sqrt{C_{D_{min}} \times \frac{C_{D_i}}{\left(C_L - C_{L_o}\right)^2}}} \tag{2}$$

in regions where C_{L_o} is 0. When the coefficients of figure 10 are used, $(L/D)_{max} = 7.4$

at Mach 2.7. The $(L/D)_{max}$ for the Boeing 2707-300 at Mach 2.7 is 7.6, according to reference 10, which is about 2 percent greater than is obtained for the airplane of this study. This difference can possibly be accounted for by the larger fuselage surface to wing-planform area ratio of the airplane of this study. At Mach 4, $(L/D)_{max} = 6.1$ for the airplane of this study. This is a decline of about 18 percent from the value obtained at Mach 2.7. This decline is about equal to that shown in reference 3 as typical for transport airplanes in general and about half that shown in reference 11 for supersonic airplanes of current technology.

Airframe Weight

Airframe weight, the operating empty weight (OEW) minus podded engine weight, was assumed for the Mach 2.7 kerosene-fueled airplane to be 1 038 200 newtons (233 312 lb). Taking the OEW of the Boeing 2707-300 prototype of June 16, 1969, from reference 10 and subtracting the estimated podded engine weight calculated by the method of this report, the OEW minus engine weight should be about 1 080 000 newtons (243 000 lb). Even though the actual airframe weight of the airplane of this study is about 4.1 percent less than that of the Boeing 2707-300, the airframe weight divided by takeoff gross weight is 0.3 percent higher at 32.7 percent for our airplane since its takeoff gross weight is less.

The maximum volume on board the airplane available for the storage of liquid methane is about 391 cubic meters (13 800 ft^3). This volume is represented by the shaded area in figure 1. Both semimonocoque and modified semimonocoque tanks with flat heads and perforated inner tie-plates (ref. 12) were used to contain the methane. According to reference 12, they have a volumetric efficiency of 95 percent and an average weight equal to 2.05 percent of the fuel weight when designed to hold 2 atmospheres gage pressure, as was the case here. For a methane capacity of 1 602 000 newtons (360 000 lb) (i.e., 391 m^3 (13 800 ft^3) and liquid methane with a density of 4090 N/m^3 (26 lb/ft^3)), this tank weight is 32 900 newtons (7400 lb). It is estimated by the method of reference 13 that the weight of fiber glass insulation surrounding the tanks must be 15 580 newtons (3500 lb) to prevent any boiloff of methane at 2 atmospheres gage pressure. The fiber glass thickness varies from tank to tank from a minimum of 0.762 centimeter (0.3 in.) to a maximum of 4.57 centimeters (1.8 in.). The total weight penalty, then, of tanks and insulation is 48 500 newtons (10 900 lb). Hence, the airframe weight of a Mach 2.7 methane-fueled airplane was assumed to be 1 087 000 newtons (244 212 lb), or about 4.7 percent more than that for the kerosene-fueled airplane. The airframe weight for this airplane, then, came to 34.3 percent of the takeoff gross weight. Since there is some uncertainty about how much the airframe weight should increase with

cruise speed, it was fixed at this value for all the methane airplanes of this study, regardless of design cruise speed. This procedure tends to produce benefits which are somewhat optimistic for the airplane designed for the higher end of the cruise speed spectrum.

Cost Estimation

Direct operating cost (DOC) is probably a better figure of merit than range, but the uncertainties of airplane pricing at this stage of development make the computational accuracy somewhat doubtful. Because of these uncertainties, the cost of all airplanes, both kerosene- and methane-fueled, was fixed at $40 million. Of this, $29.6 million was attributed to the airframe, $5.7 million to electronics, and $4.7 million to the four engines, regardless of their size or other characteristics. Time between engine overhaul was assumed to be 3000 hours. Airplane utilization was fixed at 3000 hours per year for all airplanes.

Kerosene fuel was assumed to cost 0.405 cent per newton (1.8 cents/lb) as in reference 1. Liquid methane fuel delivered to the airplane was assumed to cost 0.360 cent per newton (1.6 cents/lb) - halfway between the two suggested extremes in reference 1. The DOC was computed by the standardized method described in reference 14.

RESULTS AND DISCUSSION

Comparison of Methane with Kerosene Fuel at Mach 2.7

For the Mach 2.7 cruise case, the use of liquid methane fuel increased the range about 10.6 percent (from 6380 km (3443 n mi) to 7050 km (3808 n mi)), even though a 48 500-newton (10 900-lb) structural weight penalty was imposed for the extra weight of the methane tankage and insulation and a 6010-newton (1350-lb) penalty was imposed for the methane-air heat exchangers in the engine turbine cooling circuit. In both cases, the engine sea-level-static design airflow was 2890 newtons per second (650 lb/sec), the compressor pressure ratio was 10, the turbine-inlet temperature was 1204° C (2200° F), and the afterburner temperature was 1532° C (2790° F). No advantage was taken of the higher heat sink of the liquid methane fuel. This greater heat sink capacity can be used to lower the turbine blade metal temperature through the use of the methane-air heat exchangers in the turbine cooling circuit. In both cases, the sea-level-static thrust to gross weight ratio was about 0.348, a value somewhat higher than the minimum acceptable value of 0.327. The higher value, corresponding to a larger engine size, was used

because it maximized the range for both fuel types. The extra weight of the larger engines was more than compensated for by their greater fuel economy in both cases. Although other values of design compressor pressure ratio were not considered for kerosene fuel, it is probable that the range will maximize at the same value of pressure ratio for either fuel. The range improvement obtained by using methane will probably be about the same if subsequent results show that the optimum pressure ratio is a value other than 10.

Variation of Range with Cruise Speed for Methane-Fueled Airplanes

Figures 11 and 12 show how the range varied with respect to the cruise Mach number for various values of design compressor pressure ratio in the methane-fueled airplanes. Figure 11 shows this variation for a design turbine-inlet temperature of 1204° C (2200° F) and afterburner temperature of 1532° C (2790° F), while figure 12 shows it for a turbine-inlet temperature of 1538° C (2800° F) and an afterburner temperature of 1949° C (3540° F). Bleed air from the compressor exit for turbine cooling was fixed at 10 percent of the compressor airflow in both figures. The maximum-range envelope for these two figures is plotted in figure 13. It is obvious from this figure that only slight improvements in range are possible by increasing the cruise speed beyond Mach 2.7. In fact, as cruise speed was increased from Mach 3 to Mach 4, the range declined about 6 percent for the high-temperature engines and about 13 percent for the low-temperature engines. Hence, the higher temperature becomes more beneficial as cruise speed is increased. It provides a range advantage over the lower temperature of about 3.8 percent at Mach 2.7, 5.9 percent at Mach 3.2, and 13.2 percent at Mach 4.

Engine Parameters that Maximize Range of Methane-Fueled Airplanes

Compressor pressure ratio. - The sea-level-static design compressor pressure ratio which maximizes the range for each design cruise Mach number is shown in figure 14 for both engine temperature levels. These values were obtained from figures 11 and 12. The trend is for the optimum design compressor pressure ratio to decrease as cruise speed increases. This is understandable since at higher speeds ram compression is greater and there is less need for mechanical compression. But there is always some minimum below which the pressure ratio cannot drop if adequate low-speed performance is to be obtained. It appears from figure 14 that the minimum is 6.0 for the low-temperature engines and 6.6 for the high-temperature engines. The optimum pressure ratio is higher for the higher turbine-inlet and afterburner temperature combination. It

should be remembered that these optimum pressure ratios were computed only for the design supersonic mission. If an off-design subsonic leg had been included in the mission (to avoid overland sonic boom, for instance), the optimum pressure ratios would undoubtedly have been higher than shown here.

Airflow. - The sea-level-static design corrected airflows for these optimum engines are shown plotted against cruise Mach number in figure 15 for both engine temperatures. The flat portion of both curves at the high end of the Mach number spectrum represents cases where the engines were sized by takeoff performance with a thrust to gross weight ratio of 0.327. As design cruise speed is reduced below Mach 3.5 for the high-temperature engines, the takeoff thrust requirement no longer sizes the engines. For instance, at Mach 2.7 the range is maximized when the takeoff thrust to gross weight ratio is 0.368, a value which is 12.5 percent more than the minimum acceptable value. For a design cruise speed of Mach 2.2, the thrust-weight ratio increases still more to 0.392.

The low-temperature engines, on the other hand, are sized by the takeoff performance criterion (i.e., $F/W_g = 0.327$) until the cruise speed is reduced below Mach 2.7. At a cruise speed of Mach 2.2, the lowest value considered in this study, range is maximized with higher thrust engines. The optimum takeoff thrust to gross weight ratio for this case is 0.347.

Figure 15 can also reveal something about jet noise at the start of takeoff roll. The airflow curve for the low-temperature engines is flat beyond Mach 2.7 and the thrust-weight ratio remains constant. Hence, jet velocity, which is proportional to this ratio divided by airflow, must also be constant. Jet noise, which is a function of both the jet velocity and gas flow, should thus not be affected by designing for a higher cruise speed.

A definite increase in the takeoff jet noise will be heard if the turbine-inlet and afterburner temperatures are increased to the higher level considered in this study. Jet noise is considerably more sensitive to velocity than it is to gas flow. Hence, it will go up because of the higher jet velocities associated with the higher temperatures, despite the fact that airflow is lower. Once at the higher temperature, though, jet noise will decrease slightly as design cruise speed is increased beyond Mach 2.7. This happens because the thrust-weight ratio is declining at a faster rate than the engine airflow. Hence, jet velocity, because it is proportional to the thrust-weight ratio divided by airflow, will decline somewhat up to Mach 3.5. Takeoff jet noise should remain constant for design cruise speeds from Mach 3.5 to Mach 4.0.

Weight. - The podded engine weight is shown plotted against design cruise Mach number in figure 16. These weights are for the engines which produce the maximum ranges shown plotted in figure 13. For the low-temperature engines, the weight tends to be minimized at a cruise speed of approximately Mach 2.6. For the high-temperature engines, the weight is minimized for a cruise speed around Mach 3.0.

As cruise speed is increased from Mach 2.2 up to the point where minimum engine weight is obtained, both the design compressor pressure ratio and corrected airflow are decreasing. These decreases account for the decrease in engine weight. They more than compensate for an increasing Mach number weight factor K_M (fig. 9(a)), which tends to produce the opposite effect. But beyond Mach 2.6 for the low-temperature engines and Mach 3.0 for the high-temperature engines, the pressure ratio and airflow rates of decline either slow down or stop. Then K_M becomes the dominant factor for weight change, producing the upward trend of weight with Mach number shown in the right-hand portion of figure 16.

Since the takeoff gross weight, airframe weight, and payload were fixed in this study, there must be a tradeoff between engine weight and fuel weight. As engine weight decreases, fuel weight increases, and vice versa. Range tends to be directly proportional to fuel weight or, by the foregoing argument, inversely proportional to engine weight. In this study, other factors such as changes in engine performance and airplane aerodynamics tend to distort somewhat the inverse proportionality. Nevertheless, if the range curves of figure 13 are compared with the engine weight curves of figure 16, there is an observable trend for the range to increase when engine weight decreases and vice versa.

Variation of Airplane Cruise Flight Efficiency with Mach Number

Two other factors which affect range are the airplane lift-drag ratio L/D and the overall engine efficiency during cruise. The cruise flight efficiency (sometimes called Breguet factor) and, hence, cruise range are proportional to the product of L/D times overall engine efficiency.

Lift-drag ratio. - The ratio L/D is shown plotted against cruise Mach number in figure 17. Both actual and maximum L/D are shown. The $(L/D)_{max}$ was computed from equation (2) using the aerodynamic coefficients of figure 10. The actual L/D is less than $(L/D)_{max}$ because the actual cruise occurs at an altitude less than the aerodynamic optimum since the degree of afterburning required is lower at the lower altitude. The lower L/D is accepted as a compromise for the better specific fuel consumption obtained with less afterburning. The trend shown in figure 17 is for the L/D to decrease more rapidly as cruise speed is increased up to about Mach 3.1. Beyond this speed, the rate of decline is very nearly constant. As mentioned previously, the decline in $(L/D)_{max}$ shown in figure 17 is in agreement with that shown in reference 3 and about half that shown in reference 11. Hence, if anything, we may be predicting an $(L/D)_{max}$ which is somewhat optimistic at the high end of the cruise Mach number spectrum.

Overall engine efficiency. - The overall engine efficiency is shown plotted against cruise Mach number for both engine temperatures in figure 18. This efficiency, which is proportional to the product of specific impulse times Mach number, increased linearly with cruise Mach number for the optimized engines up to Mach 3.2, but then the rate of increase began to slacken for the lower turbine-inlet and afterburner temperature combination. Nevertheless, the efficiency was still increasing with Mach number at Mach 4. The rate of increase hardly slackened at all for the higher turbine-inlet and afterburner temperature combination as cruise speed was increased up to Mach 4.

Flight efficiency. - The relative flight efficiencies during cruise are shown plotted against cruise Mach number in figure 19. They were obtained by first multiplying the actual L/D's of figure 17 by the overall engine efficiencies of figure 18, and then dividing by the product thus obtained at Mach 2.7 with low-temperature engines.

The cruise flight efficiencies for both turbine temperatures maximize at Mach numbers higher than those at which the total range is maximized. Other factors such as the amount of fuel consumed during takeoff, climb-acceleration, letdown, hold, etc. may tend to modify the picture presented by the cruise flight efficiency by itself. But perhaps the most important other factor is the engine weight effect, which was discussed in connection with figure 16. Because of the weight tradeoff between engine weight and fuel, range tends to be maximized for a cruise Mach number where engine weight is a minimum. Engine weight is minimized at a Mach number lower than that at which cruise flight efficiency is maximized. Hence, in retrospect, it is logical that total range (fig. 13) is maximized at a cruise speed between the engine-weight and flight-efficiency optimums.

The cruise flight efficiency curves of figure 19 also show that from Mach 2.7 to Mach 3.5 turbine-inlet temperature is unimportant. The range curves of figure 13, however, show that over this interval the high-temperature engines produce ranges from 150 to 300 nautical miles (278 to 556 km) greater than the low-temperature engines. This, too, is the result of the engine-weight effect. Engine weight is reduced by 28 500 to 62 300 newtons (6400 to 14 000 lb) when the high-temperature engine is used over the cruise speed interval from Mach 2.7 to Mach 3.5.

Cruise Sonic Boom

Although the flight path used in this study was not chosen to minimize sonic boom, the far-field sonic boom at the beginning of cruise, as calculated by the method of reference 15, declined with Mach number as shown in figure 20. For example, the initial cruise boom on the ground decreases from 93.4 to 83.8 newtons per square meter (1.95 to 1.75 lb/ft^2) as the cruise speed is increased from Mach 2.7 to Mach 3.2. If cruise

speed is increased still further to Mach 4, the initial cruise boom decreases to 71.9 newtons per square meter (1.50 lb/ft^2). Although the climb sonic boom changes very little as cruise Mach number is increased, the reduction in cruise sonic boom may be of some importance because of the long range covered during cruise. The lower level of cruise boom obtained at the higher Mach numbers is both the result of extra distance between the airplane and the ground observer when he perceives the shock and the lower C_L requirement. It should be emphasized that the sonic boom calculations made here are for the far-field N-shaped wave. At the lower cruise Mach numbers where the altitude is lower, near-field effects may change the shape of the wave and reduce the maximum amplitude from the levels shown in figure 20.

Block Time

Other criteria besides range exist for judging the benefits of higher cruise speed. Block time, the airport-to-airport trip time, is such a criterion and is shown plotted against cruise Mach number in figure 21 for a constant 7408-kilometer- (4000-n-mi) range. A 15-minute taxi time is added to the actual flight time in these block time calculations. It can be seen from figure 21 that a half-hour saving in block time is obtained by increasing the cruise speed from Mach 2.2 to Mach 2.7. If cruise speed is increased to Mach 3.2, block time is further reduced by about 20 minutes. Another 20-minute saving occurs if cruise speed is increased to Mach 4.0. The block times shown in figure 21 do not exactly correspond to the block times obtained when range is allowed to vary (e.g., as in fig. 13), but the trend is more easily understood with a fixed range. To obtain a constant range with a fixed takeoff gross weight, as assumed in figure 21, payload must be allowed to fluctuate with design cruise Mach number.

Direct Operating Cost

As mentioned earlier, DOC is probably a better indicator of the advantage of higher cruise speed than either range or block time. Unfortunately, at this stage of development, certain costs are so uncertain that accurate computation of DOC is practically impossible. Nevertheless, calculations were made and certain trends can be determined.

Comparison of methane with kerosene fuel at Mach 2.7. - For the Mach 2.7 cruise case, the use of methane fuel reduced the DOC by 11.5 percent from 0.762 to 0.674 cent per seat kilometer (1.225 to 1.084 cents/seat - s mi). In both cases the engine sea-level-static design airflow was 2890 newtons per second (650 lb/sec), design compressor pressure ratio was 10, turbine-inlet temperature was 1204° C (2200° F), and maxi-

mum afterburner temperature was 1532° C (2790° F). No advantage was taken of the higher heat sink available with liquid methane in these calculations. Although a comparison of the DOC improvement to be gained with methane instead of kerosene fuel was not made at any other design compressor pressure ratio, the improvement very likely would be about the same although the absolute values of DOC would change.

Effect of cruise Mach number on methane-fueled airplanes. - Figure 22 is a plot of DOC against cruise Mach number for the low-temperature methane-fuel engines at each of the design compressor pressure ratios considered in this study. This figure corresponds to figure 11 where range was used as the figure of merit. The fact that block time continues to decline as cruise Mach number increases counteracts some of the range decline to produce a DOC which optimizes at a cruise Mach number greater than the value indicated by figure 11. Figure 23 is a similar plot of DOC against cruise Mach number for the higher-temperature engines. It corresponds to the range curves shown in figure 12. Figure 24 is a plot of the minimum DOC envelope of the curves of figures 22 and 23. It is apparent from figure 24 that the DOC minimizes for a design cruise speed of about Mach 3.5 for the low-temperature engines and Mach 4.0 for the high-temperature engines. The minimum DOC for the low-temperature engines is 0.612 cent per seat kilometer (0.985 cent/seat - s mi), while for the high-temperature engines it is 0.587 cent per seat kilometer (0.945 cent/seat - s mi). Most of the possible DOC improvement, though, was obtained at a design cruise Mach number of 3.2, where a 20-minute saving in block time and practically no range change combine to produce a DOC about 7 percent below that obtainable at Mach 2.7 with methane. At Mach 3.2, the DOC was 0.622 cent per seat kilometer (1.00 cent/seat - s mi), for the low-temperature engines and 0.609 cent per seat kilometer (0.980 cent/seat - s mi) for the high-temperature engines. Although figure 24 shows there is some gain possible by increasing the cruise Mach number beyond 3.2, it should be remembered that it was optimistically assumed that the percentage of compressor discharge air bled to the turbine for cooling, airframe weight, and airplane cost did not increase as cruise Mach number was increased. Therefore, it is unlikely that very much of the gain shown beyond Mach 3.2 can actually be obtained.

Figure 24 also shows that as the cruise Mach number increases, the advantage of higher engine temperature increases. For instance, at Mach 2.7 use of the higher temperature reduces the DOC about 1 percent, but at Mach 3.2 a 2-percent reduction is possible. At Mach 4.0, use of the high-temperature engines reduces the DOC about 5 percent.

If the Mach 3.2 methane-fueled airplane is compared with a Mach 2.7 kerosene-fueled airplane with optimized engines, it is estimated that DOC would be reduced 17 to 18 percent, depending on the turbine-inlet temperature of the methane engines. The

kerosene engines were assumed to have a turbine-inlet temperature of 1204° C (2200° F) in this comparison.

CONCLUDING REMARKS

Increasing the speed of an SST would be expected to improve its cruise range which is directly proportional to Mach number (among other factors). A major factor preventing cruise speeds higher than the present maximum of Mach 2.7 is the limited heat sink of conventional kerosene-type fuels. A fuel such as liquid methane has up to seven times the heat sink of conventional fuels and thus might be considered for cruise speeds beyond Mach 2.7. In the present study, range and the corresponding direct operating cost (DOC) were computed for a fixed-wing methane-fueled airplane for a range of cruise speeds up to Mach 4. These 285-passenger airplanes had their takeoff gross weights fixed at 3 170 000 newtons (712 000 lb) in this comparison.

If the methane is substituted for kerosene fuel at Mach 2.7, both range and DOC are improved by about 11 percent despite the extra fuel tank and insulation weight aboard the methane airplane. Both airplanes had equal payloads, takeoff gross weights, and turbine-inlet temperatures.

Only slight improvements in range were obtained by increasing the cruise speed of the methane-fueled airplanes beyond Mach 2.7. Range maximized near Mach 3 and then declined 13 percent when turbine-inlet and afterburner temperatures were fixed at the levels used in the Mach 2.7 conventionally fueled engines. Some of the assumptions made in this study favor high speeds, but even with this built-in bias the range declined with increases in speed beyond Mach 3.

Direct operating cost reductions were obtained with increases in cruise speed because of the beneficial effect of lower trip time. But most of the possible DOC improvement was obtained at a cruise speed of Mach 3.2, where a 20-minute time saving and practically no range change combine to provide a DOC about 7 percent below that obtained at Mach 2.7. If the Mach 3.2 methane airplane is compared to the Mach 2.7 kerosene-fueled airplane, DOC is reduced about 17 percent. For the methane airplanes, the DOC reaches a minimum near Mach 3.5, where it is 8.4 percent lower than at Mach 2.7.

Besides the higher cruise Mach numbers, the greater heat sink of methane may also allow higher turbine-inlet and afterburner temperatures to be used. The cold methane fuel could be used to precool the turbine cooling air enough so that the gas temperature could be raised without damaging or shortening the life of the turbine blades. The higher temperatures proved to be most beneficial at the higher Mach numbers. The higher temperatures used in this study provide a range improvement of 3.8 percent at Mach 2.7, 5.9 percent at Mach 3.2, and 13.2 percent at Mach 4, relative to the lower-temperature

methane-fuel engines. The higher temperatures also cause reductions in DOC, especially at the higher Mach numbers. For instance, at Mach 2.7, the higher temperatures reduce DOC by only 1 percent, but at Mach 4 a reduction of 5 percent is possible.

In addition to the modest improvements in trip time and DOC, the higher speed lowers the initial cruise sonic boom because of both the extra attenuation resulting from a higher altitude and the lower lift coefficient. For instance, the far-field sonic boom on the ground was calculated to decrease from 93.4 to 71.9 newtons per square meter (1.95 to 1.50 lb/ft^2) as cruise speed was increased from Mach 2.7 to Mach 4.0.

Higher cruise speeds do not have much effect on the level of takeoff noise, except that the high-temperature engines which are desirable for high speeds are noisier than the low-temperature engines.

Many assumptions were made to obtain the results for the higher Mach numbers described in this report. In areas where data were available, the assumptions were based on these data. An example is the rising trend of podded engine weight with increasing Mach number. In other areas, where less data were available, however, assumptions were made which should favor higher speeds. This exemplifies the philosophy of this report -- that is, to give the higher Mach number the benefit of the doubt. For example, the airframe weight (i.e., the operating empty weight minus podded engines) and cost of the entire airplane were assumed to remain constant as design cruise speed was increased. These are certainly optimistic assumptions. The amount of compressor discharge bleed air used for turbine cooling was kept constant as cruise speed was increased. Since a good argument could be made for increasing the cooling bleed with speed, this too is an optimistic assumption. The assumed rise in the coefficient of induced drag due to lift with increasing Mach number is considerably less than is indicated by theory for a slender, thin-delta wing with no favorable leading-edge suction forces. This assumption tends to produce optimistic lift-drag ratios at the higher Mach numbers.

The results of this study are for a particular type of configuration only. Furthermore, the airplane was sized to provide a range in the vicinity of 7408 kilometers (4000 n mi). It is possible that airplanes sized for greater ranges might derive more benefit from higher cruise speeds. It is possible, too, that other configurations might show more promise. But the advantages of cruise speeds much higher than Mach 3.2 do not presently appear to be too exciting based on the results of this study.

Lewis Research Center,
National Aeronautics and Space Administration,
Cleveland, Ohio, January 28, 1971,
720-03.

REFERENCES

1. Whitlow, John B., Jr.; Eisenberg, Joseph D.; and Shovlin, Michael D.: Potential of Liquid-Methane Fuel for Mach 3 Commercial Supersonic Transports. NASA TN D-3471, 1966.

2. Weber, Richard J.; Dugan, James F., Jr.; and Luidens, Roger W.: Methane-Fueled Propulsion Systems. Paper 66-685, AIAA, June 1966.

3. Sutcliffe, P. L.: The General Problem. Supersonic Engineering. J. T. Henshaw, ed., John Wiley & Sons, Inc., 1962, pp. 6-9.

4. Plattner, C. M.: Noise, Traffic Loom as Key SST Problems. Aviation Week & Space Tech., vol. 89, no. 24, Dec. 9, 1968, pp. 21-23.

5. Dugan, James F., Jr.: Compressor and Turbine Matching. Aerodynamic Design of Axial-Flow Compressors. Irving A. Johnsen and Robert O. Bullock, eds. NASA SP-36, 1965, pp. 469-508.

6. Anon.: Boeing's Latest SST Proposal. Part One. Flight International, vol. 95, no. 3123, Jan. 16, 1969, pp. 104-108.

7. Gerend, Robert P.; and Roundhill, John P.: Correlation of Gas Turbine Engine Weights and Dimensions. Paper 70-699, AIAA, June 1970.

8. Koenig, Robert W.; and Kraft, Gerald A.: Influence of High-Turbine-Inlet-Temperature Engines in a Methane-Fueled SST When Takeoff Jet Noise Limits are Considered. NASA TN D-4965, 1968.

9. Furness, B.: Basic Aerodynamics. Supersonic Engineering. J. T. Henshaw, ed., John Wiley & Sons, Inc., 1962, pp. 104-107.

10. Swan, Walter C.: A Review of the Configuration Development of the U. S. Supersonic Transport. Aircraft Eng., vol. 41, Oct. 1969, pp. 10, 12-16.

11. Bisplinghoff, Raymond L.: Supersonic and Hypersonic Flight. Bioastronautics and the Exploration of Space. Charles H. Roadman, Hubertus Strughold, and Roland B. Mitchell, eds. School of Aerospace Medicine, Nov. 1968, pp. 95-111. (Available from DDC as AD-687893.)

12. Chambellan, Rene E.; and Bevevino, William A.: Comparative Study of Fuselage Tanks for Liquid-Methane-Fueled Supersonic Aircraft. NASA TN D-4837, 1968.

13. Eisenberg, Joseph D.: High-Energy Fuels for Supersonic Transport Reserves. NASA TN D-3987, 1967.

14. Anon.: Standard Method of Estimating Direct Operating Costs of Transport Airplanes. Air Transport Association of Am., Aug. 1960.

15. Whitlow, John B., Jr.: Airplane Size and Staging Effects on SST Cruise Sonic Boom. NASA TN D-4677, 1968.

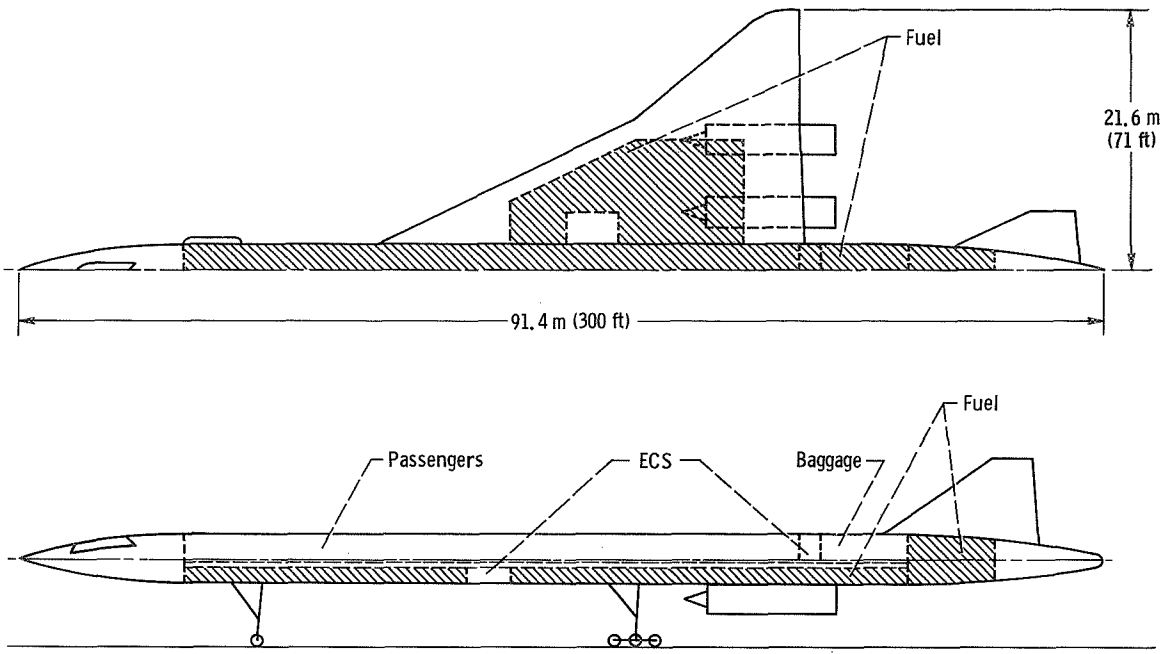

Figure 1. - Layout of a methane-fueled SST designed for maximum cruise speed of Mach 4.0. Passenger capacity, 285; fuel capacity, 390 cubic meters (13 800 ft^3).

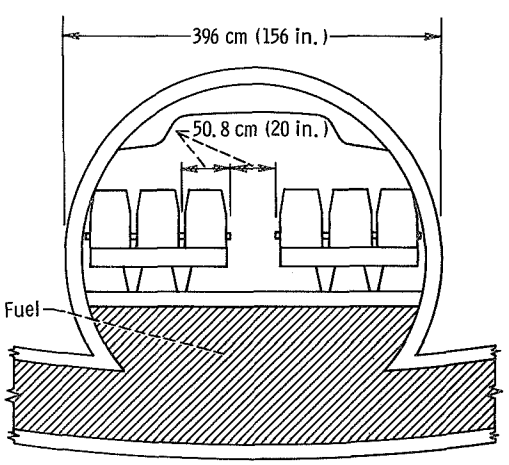

Figure 2. - Typical fuselage section at 35-percent wing chord.

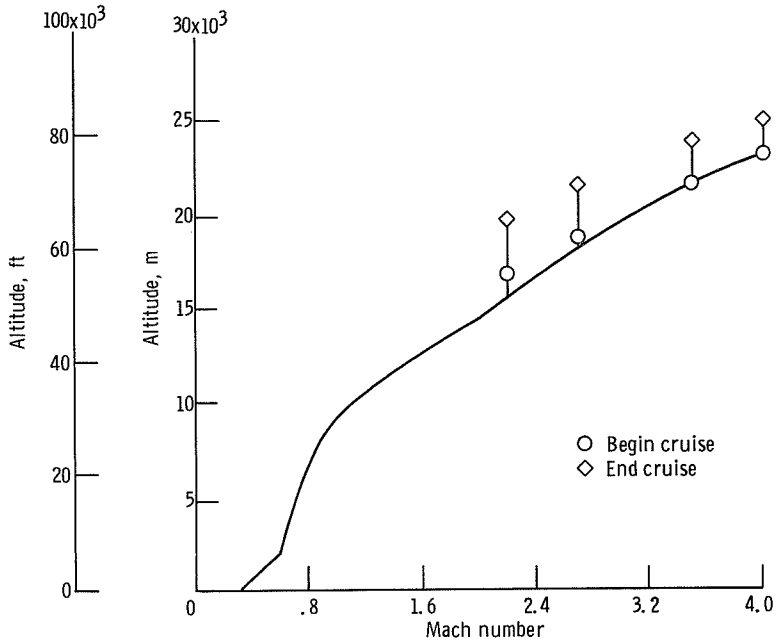

Figure 3. - Flight profile for climb, acceleration, and cruise.

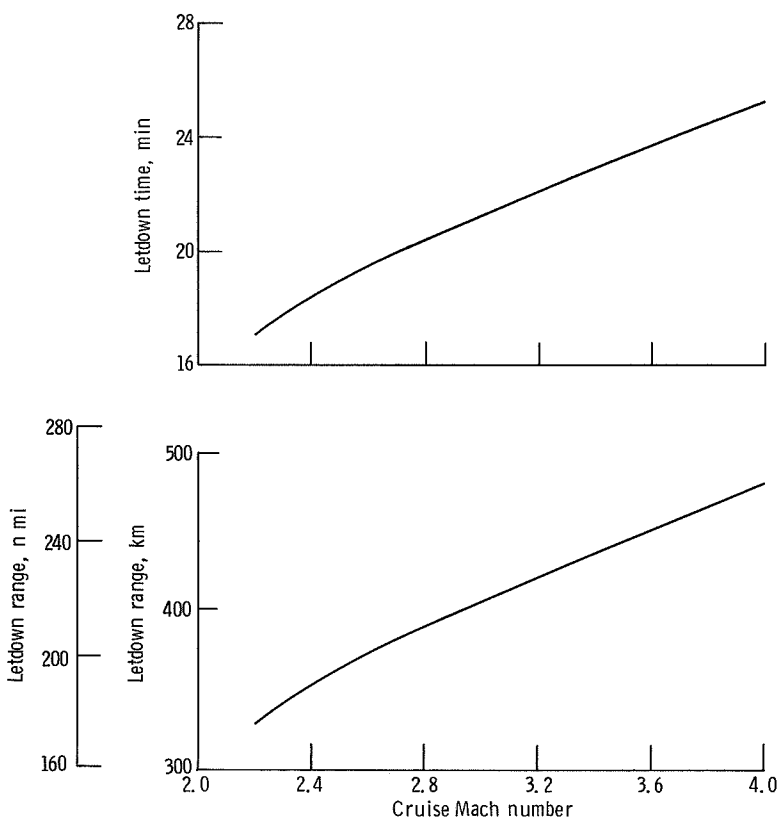

Figure 4. - Assumed schedule of letdown time and range as function of cruise Mach number.

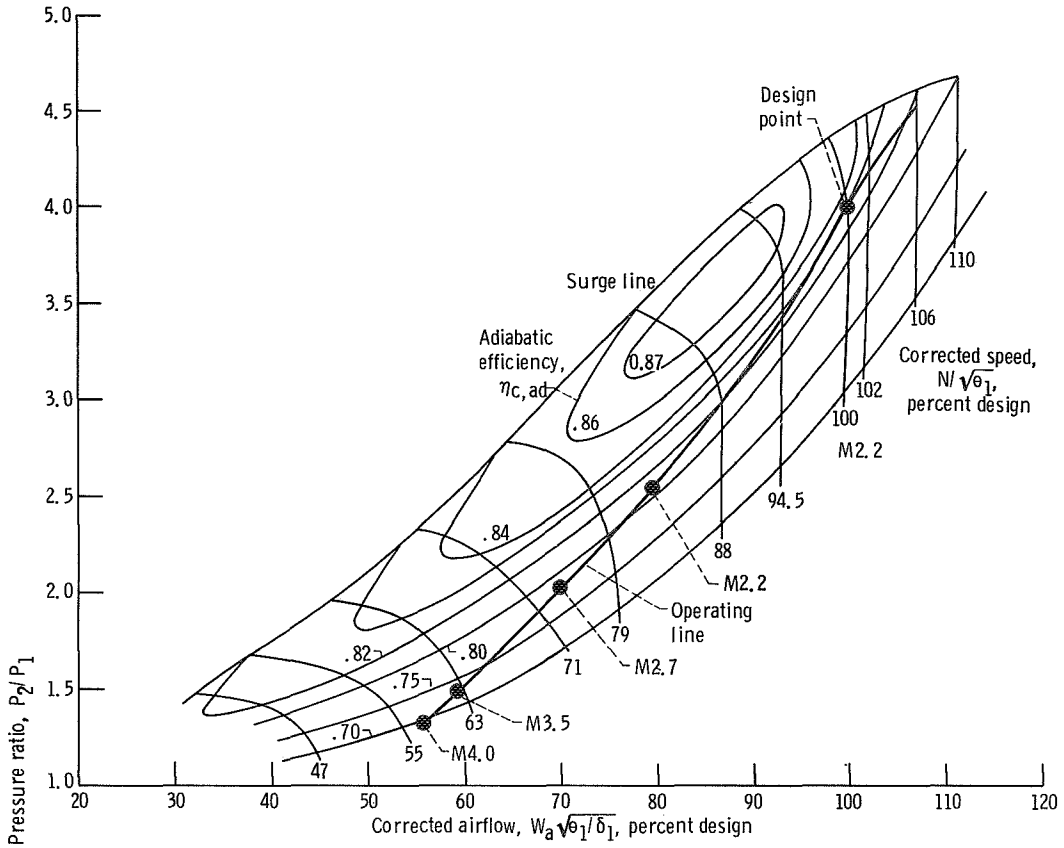

(a) Design pressure ratio of 4.

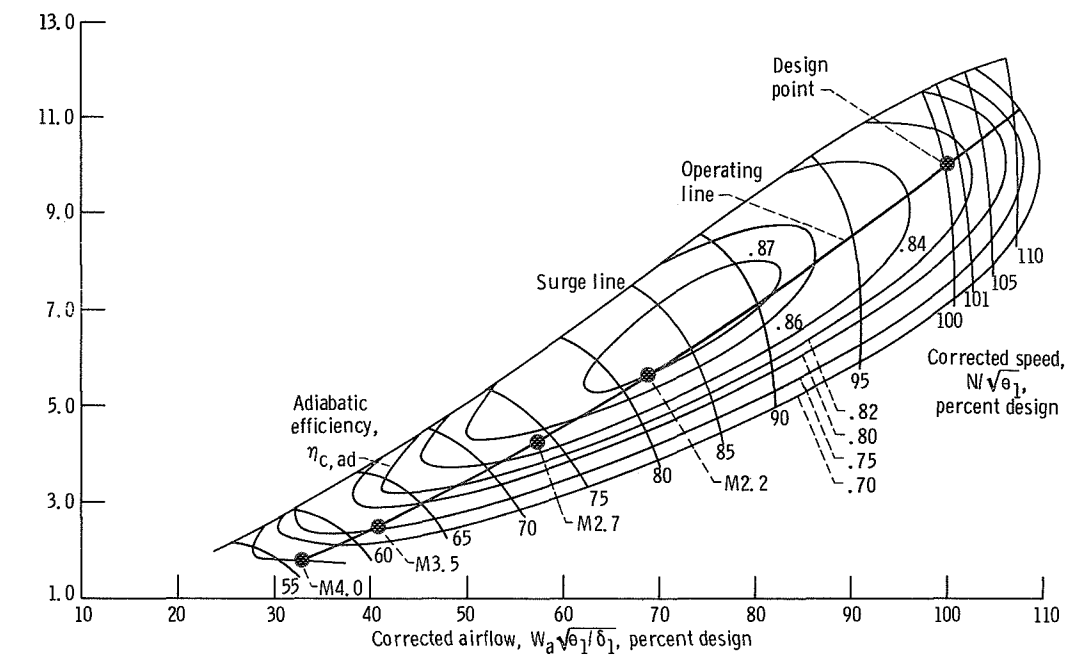

(b) Design pressure ratio of 10.

Figure 5. - Typical compressor maps used in this study. Operating lines shown result from matching compressor with its driving turbine holding shaft speed N constant and turbine inlet temperature fixed at design.

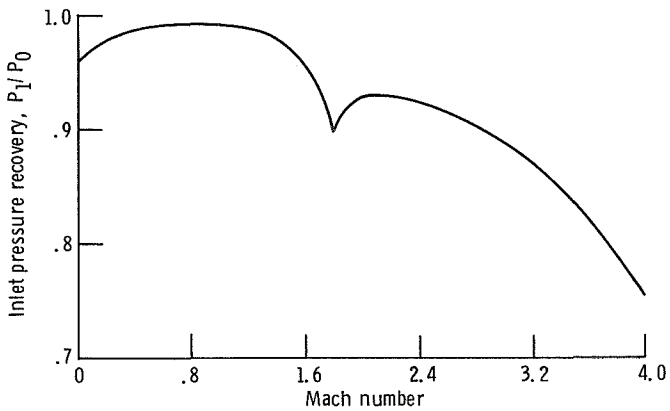

Figure 6. - Inlet pressure recovery schedule.

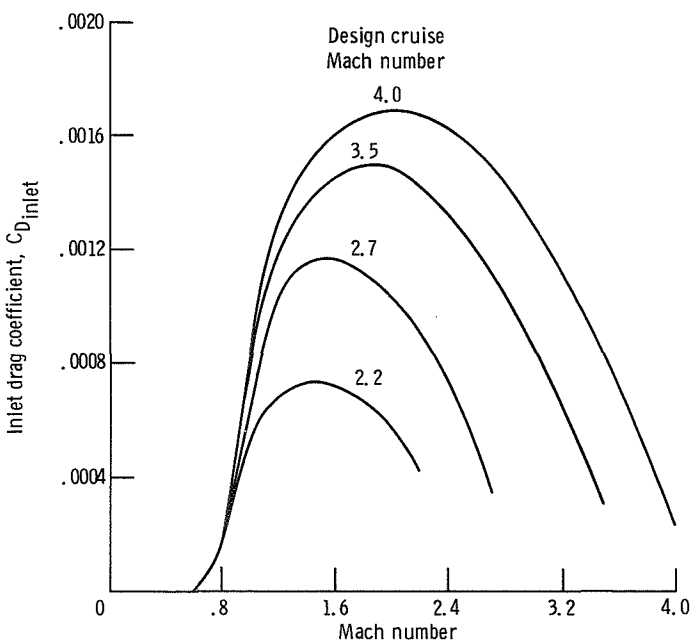

Figure 7. - Assumed schedule of inlet drag coefficient as function of Mach number for four 3960 newton per second (666 lb/sec) afterburning turbojet engines. Coefficient based on S_{ref} = 716 square meters (7700 ft^2). Can be adjusted for other engine sizes by multiplying by the quotient of the new design airflow divided by the reference airflow.

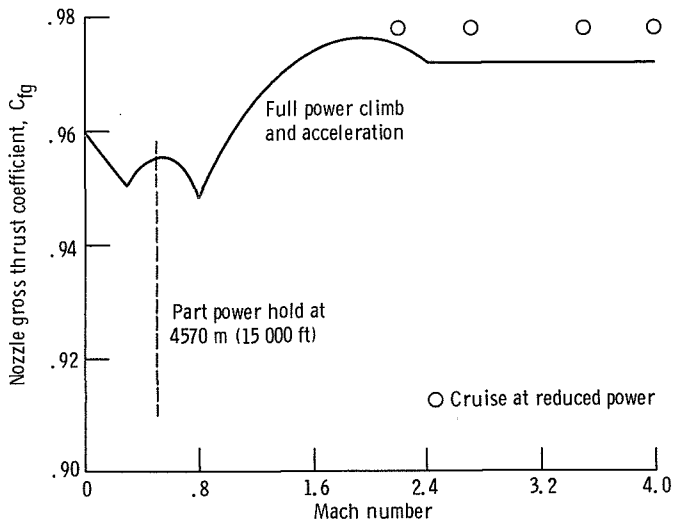

Figure 8. - Schedule of nozzle gross thrust coefficient as function of freestream Mach number. Boattail drag included.

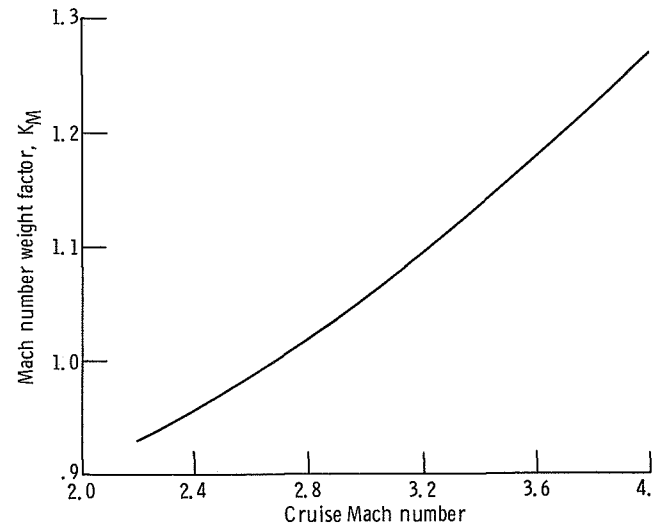

(a) Cruise Mach number weight factor.

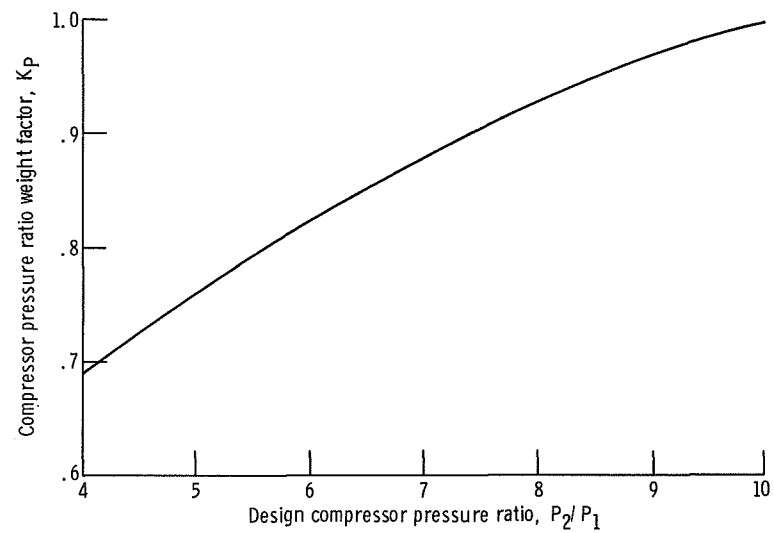

(b) Compressor pressure ratio weight factor.

Figure 9. - Effect of design parameters on engine weight factors used in equation (1).

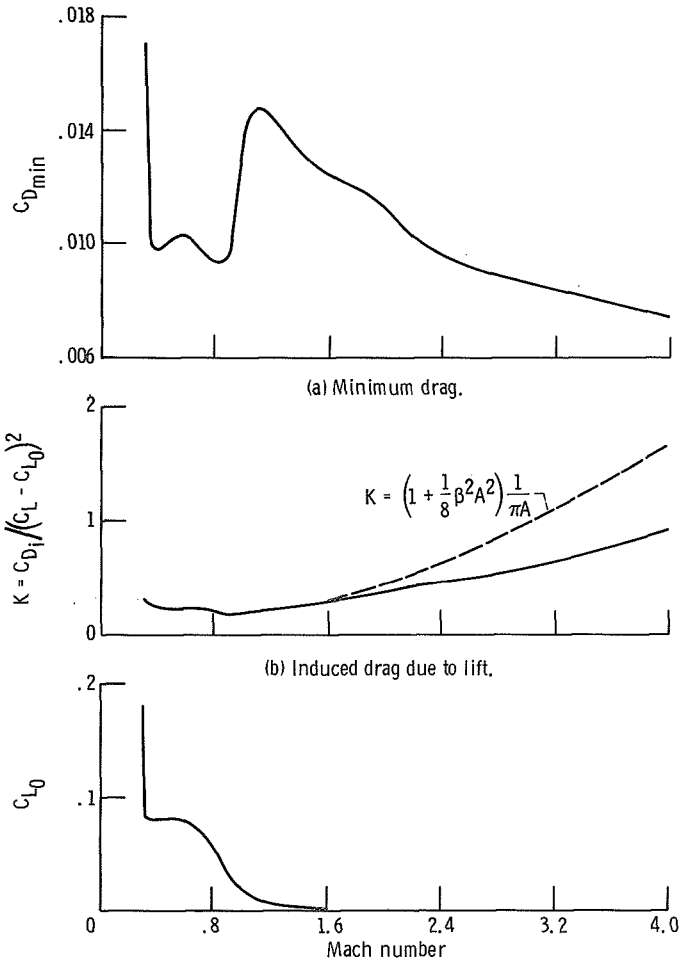

Figure 10. - Aerodynamic coefficients based on S_{ref} = 716 square meters (7700 ft^2).

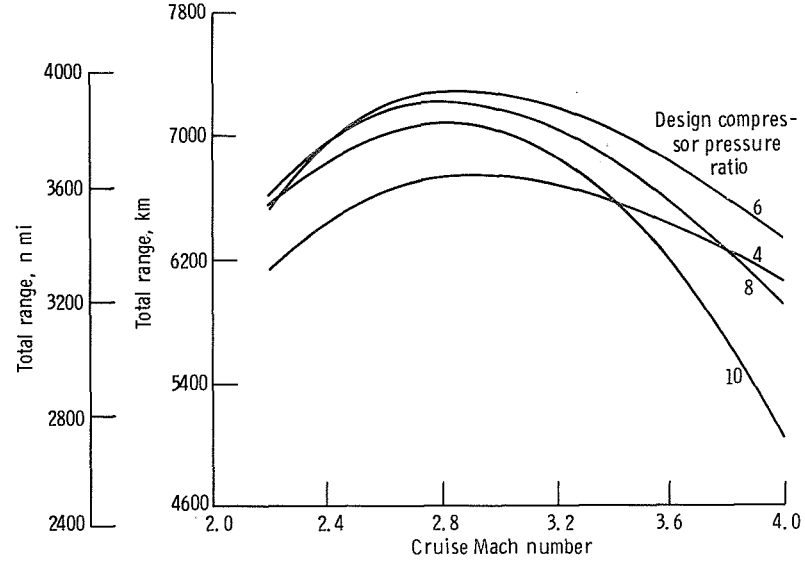

Figure 11. - Range as function of design cruise Mach number for methane fueled afterburning turbojet engines with various design compressor pressure ratios. Turbine inlet temperature, 1204° C (2200° F); takeoff gross weight, 3 170 000 newtons (712 000 lb); payload, 265 000 newtons (59 600 lb) (285 passengers).

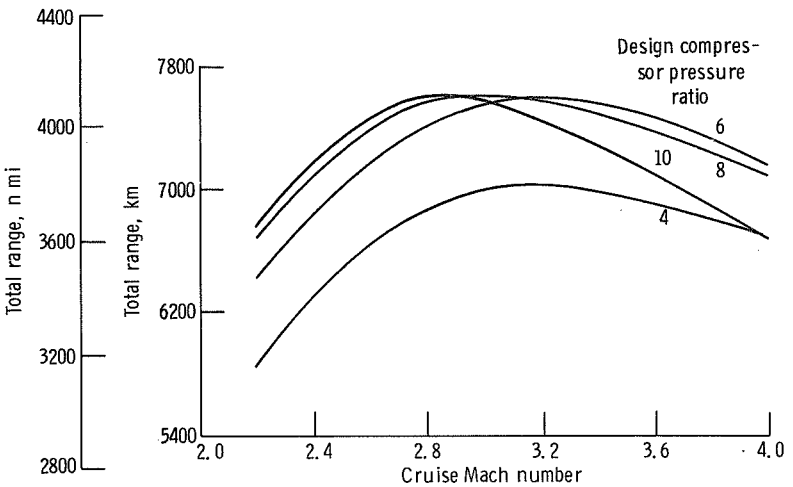

Figure 12. - Range as function of design cruise Mach number for methane-fueled afterburning turbojet engines with various design compressor pressure ratios. Turbine inlet temperature, 1538° C (2800° F); takeoff gross weight, 3 170 000 newtons (712 000 lb); payload, 265 000 newtons (59 600 lb) (285 passengers).

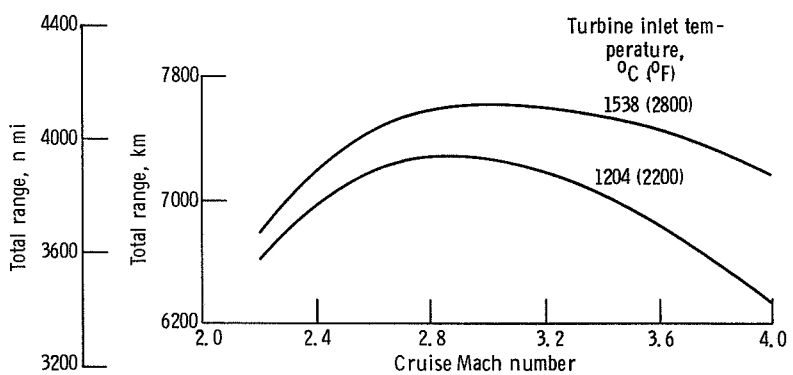

Figure 13. - Range as function of design cruise Mach number for methane-fueled afterburning turbojet engines with optimized design compressor pressure ratios. Takeoff gross weight, 3 170 000 newtons (712 000 lb); payload, 265 000 newtons (59 600 lb) (285 passengers).

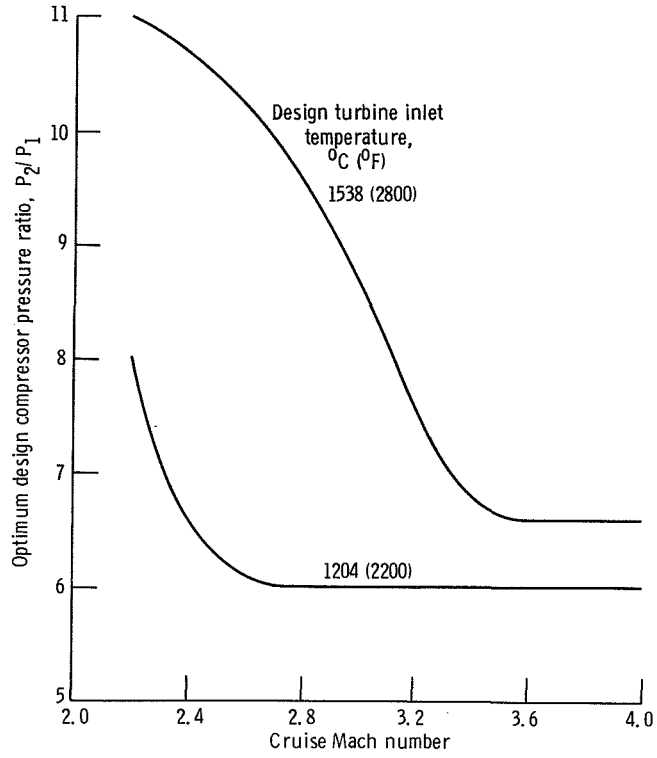

Figure 14. - Optimum design compressor pressure ratio as a function of cruise Mach number for afterburning turbojet engines with 10-percent compressor discharge air bleed chargeable to cycle for turbine cooling. Methane fuel.

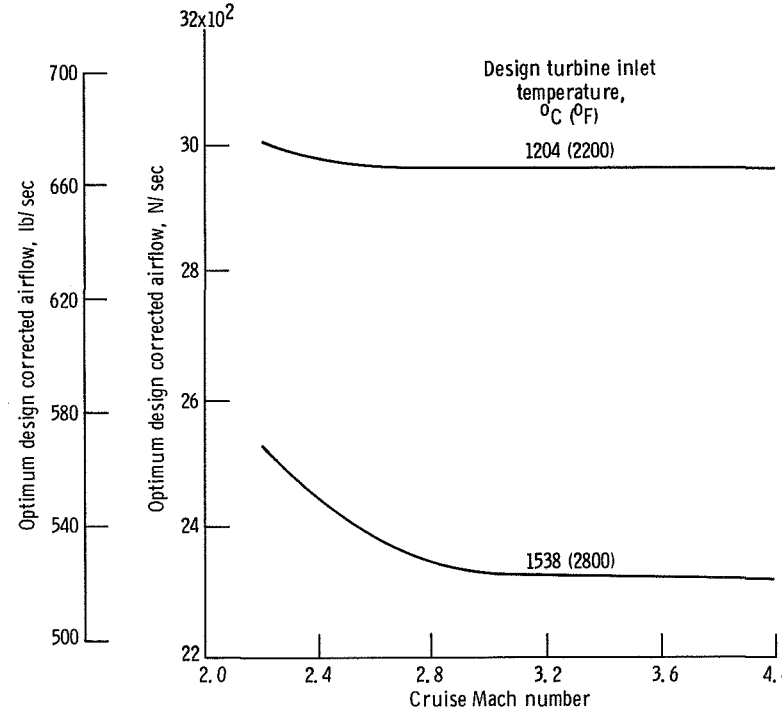

Figure 15. - Optimum design corrected airflow at compressor face as function of cruise Mach number for afterburning turbojet engines with 10-percent compressor discharge air bleed chargeable to cycle for turbine cooling. Methane fuel.

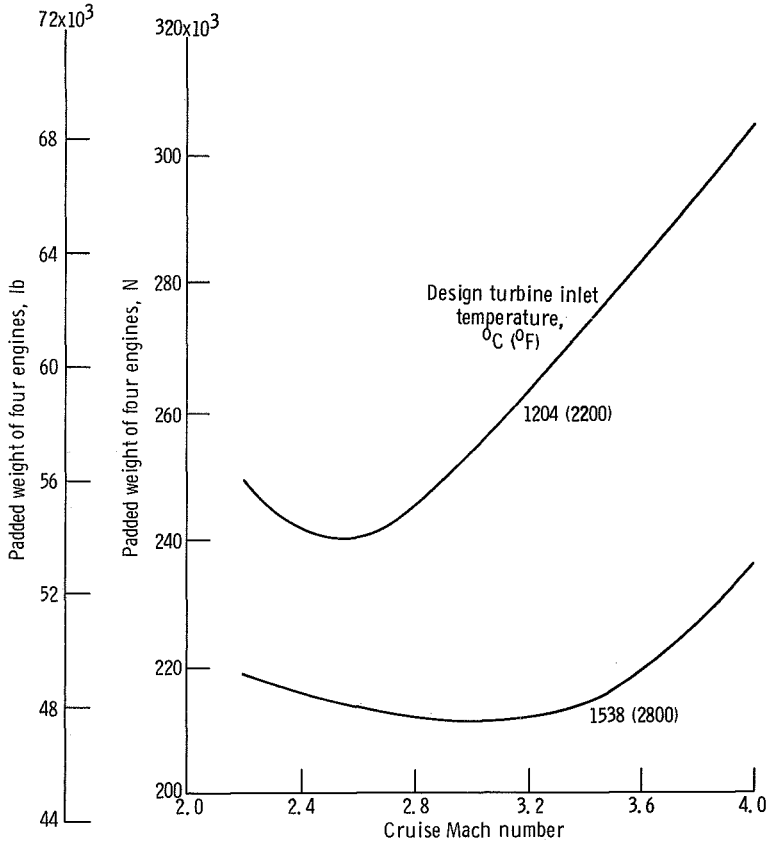

Figure 16. - Engine weight of four optimized afterburning turbojets as function of Mach number. Methane fuel; takeoff gross weight, 3 170 000 newtons (712 000 lb).

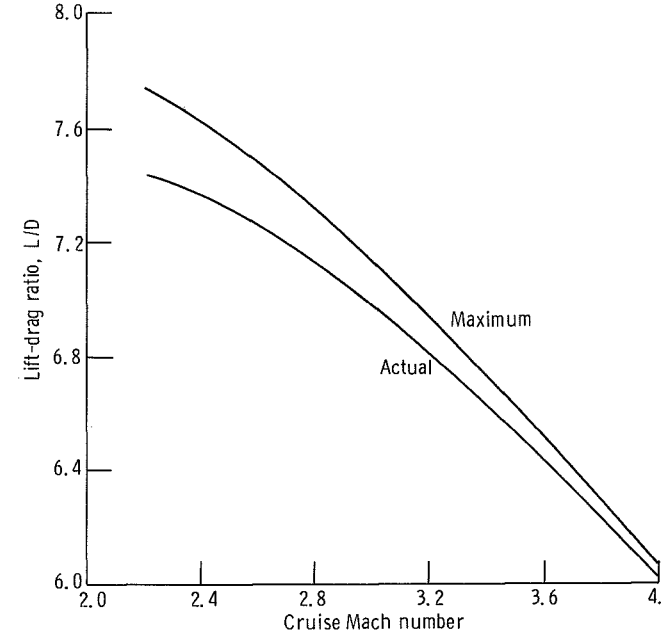

Figure 17. - Cruise lift-drag ratio as function of Mach number. Methane fuel; takeoff gross weight, 3 170 000 newtons (712 000 lb); payload, 265 000 newtons (59 600 lb) (285 passengers).

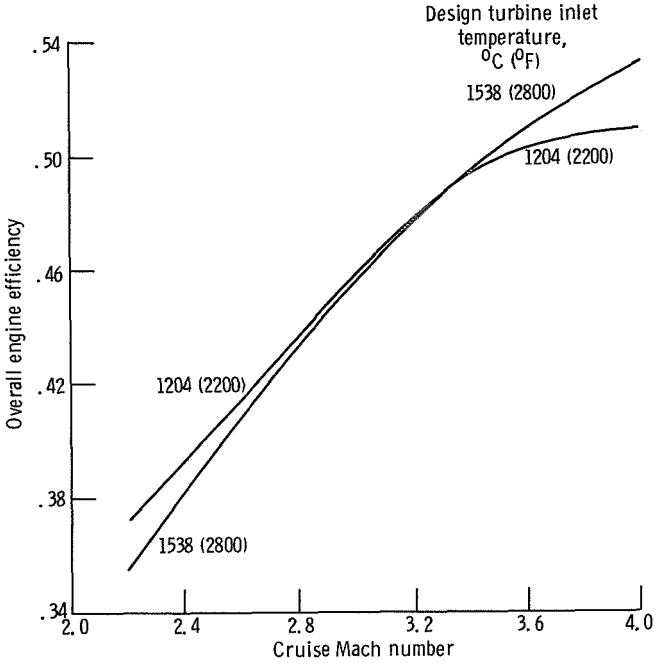

Figure 18. - Cruise overall engine efficiency as function of design cruise Mach number for methane-fueled afterburning turbojet engines optimized for maximum range.

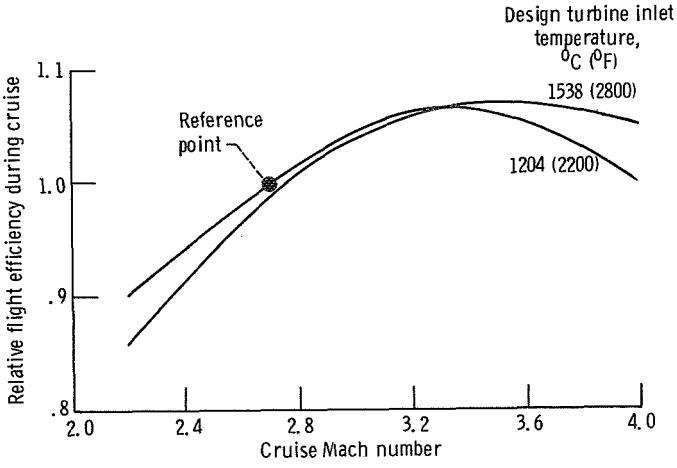

Figure 19. - Relative flight efficiency during cruise as function of design cruise Mach number for methane-fueled afterburning turbojet engines optimized for maximum range. Flight efficiency proportional to product of airplane L/D times engine overall efficiency.

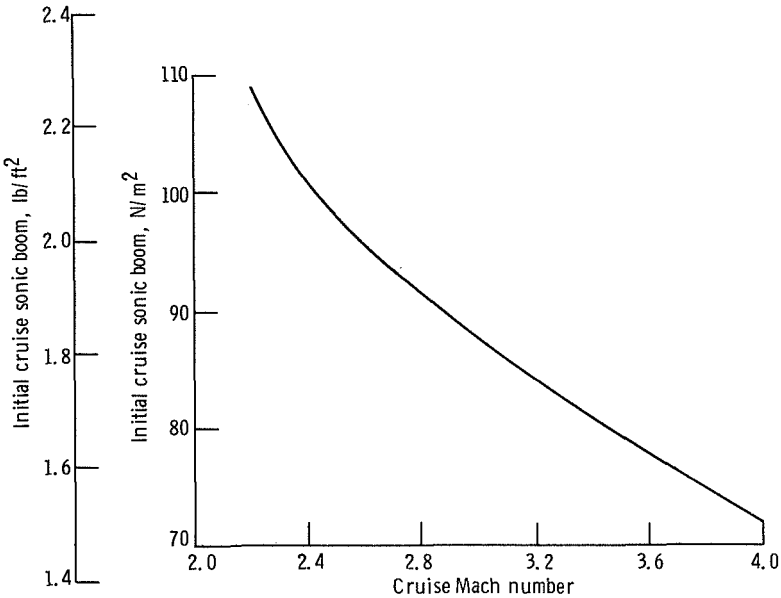

Figure 20. - Far-field sonic boom at start of cruise as function of design cruise Mach number. Methane fuel; takeoff gross weight, 3 170 000 newtons (712 000 lb); payload, 265 000 newtons (59 600 lb) (285 passengers).

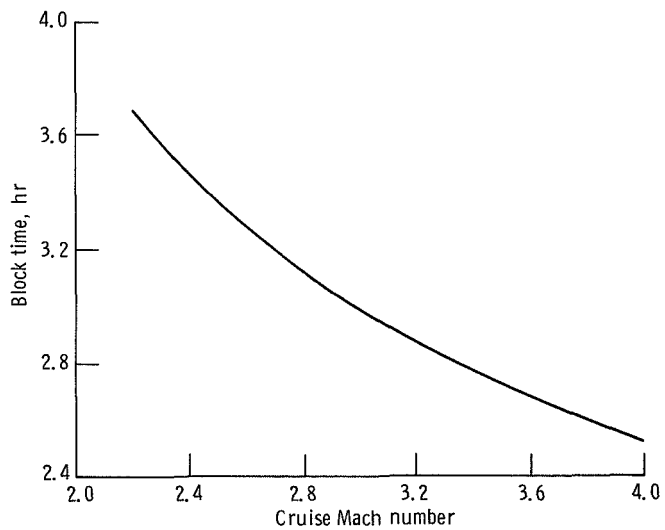

Figure 21. - Block time for constant 7408-kilometer (4000 n mi) range as function of cruise Mach number; optimized methane-fueled afterburning turbojets; takeoff gross weight, 3 170 000 newtons (712 000 lb); variable payload.

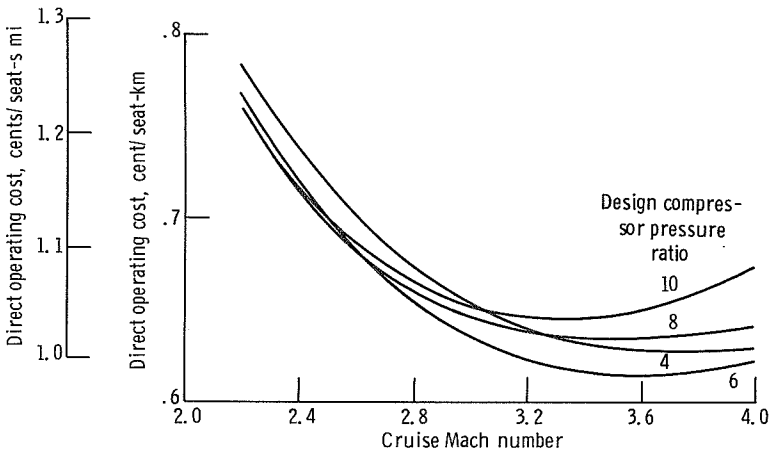

Figure 22. - Direct operating cost as function of cruise Mach number for methane-fueled afterburning turbojet engines with various design compressor pressure ratios. Turbine inlet temperature, 1204° C (2200° F); takeoff gross weight, 3 170 000 newtons (712 000 lb); payload, 265 000 newtons (59 600 lb) (285 passengers); methane fuel, 0.359 cent per newton (1.6 cents/ lb); airplane cost, $40 million.

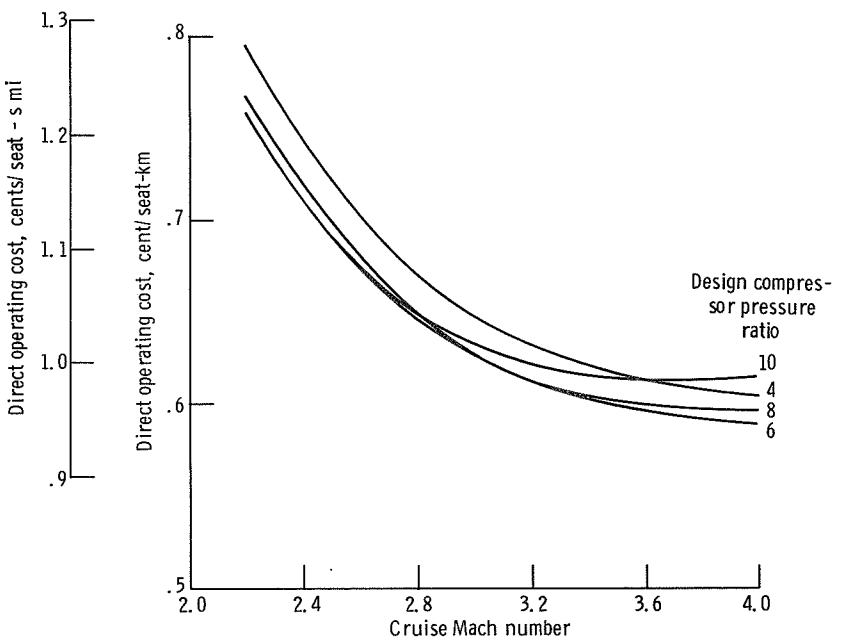

Figure 23. - Direct operating cost as function of cruise Mach number for methane-fueled afterburning turbojet engines with various design compressor pressure ratios. Turbine inlet temperature, 1538° C (2800° F); takeoff gross weight, 3 170 000 newtons (712 000 lb); payload, 265 000 newtons (59 600 lb); methane fuel, 0.359 cent per newton (1.6 cents/ lb); airplane cost, $40 million.

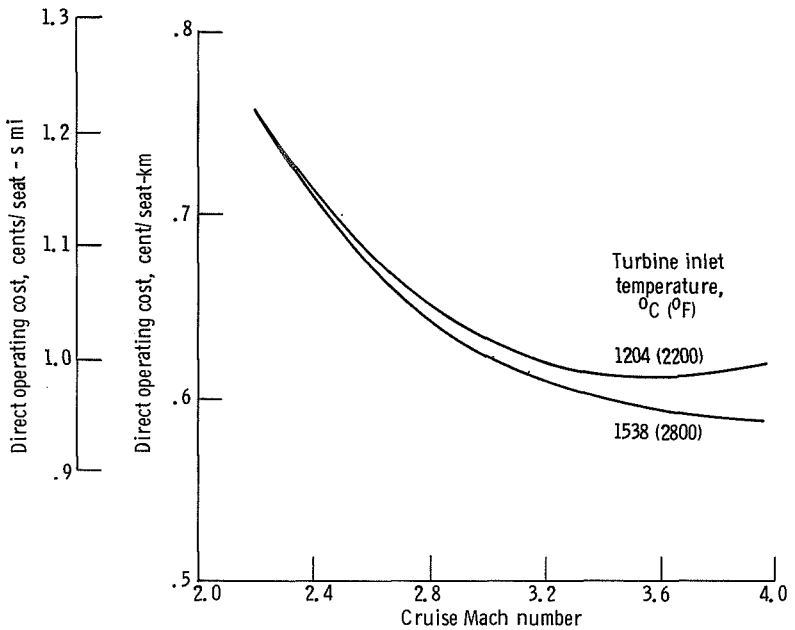

Figure 24. - Direct operating cost as function of cruise Mach number for methane-fueled afterburning turbojet engines with optimized design compressor pressure ratios. Take-off gross weight, 3 170 000 newtons (712 000 lb); payload, 265 000 newtons (59 600 lb); (285 passengers); methane fuel, 0.359 cent per newton (1.6 cents/ lb); airplane cost, $40 million.

NASA-Langley, 1971 —— 2 E-6088

"The aeronautical and space activities of the United States shall be conducted so as to contribute . . . to the expansion of human knowledge of phenomena in the atmosphere and space. The Administration shall provide for the widest practicable and appropriate dissemination of information concerning its activities and the results thereof."

—NATIONAL AERONAUTICS AND SPACE ACT OF 1958

NASA SCIENTIFIC AND TECHNICAL PUBLICATIONS

TECHNICAL REPORTS: Scientific and technical information considered important, complete, and a lasting contribution to existing knowledge.

TECHNICAL NOTES: Information less broad in scope but nevertheless of importance as a contribution to existing knowledge.

TECHNICAL MEMORANDUMS: Information receiving limited distribution because of preliminary data, security classification, or other reasons.

CONTRACTOR REPORTS: Scientific and technical information generated under a NASA contract or grant and considered an important contribution to existing knowledge.

TECHNICAL TRANSLATIONS: Information published in a foreign language considered to merit NASA distribution in English.

SPECIAL PUBLICATIONS: Information derived from or of value to NASA activities. Publications include conference proceedings, monographs, data compilations, handbooks, sourcebooks, and special bibliographies.

TECHNOLOGY UTILIZATION PUBLICATIONS: Information on technology used by NASA that may be of particular interest in commercial and other non-aerospace applications. Publications include Tech Briefs, Technology Utilization Reports and Technology Surveys.

Details on the availability of these publications may be obtained from:

SCIENTIFIC AND TECHNICAL INFORMATION OFFICE

NATIONAL AERONAUTICS AND SPACE ADMINISTRATION

Washington, D.C. 20546